



COMPARISON OF GEODETIC AND GLACIOLOGICAL MASS
BALANCE ON GULKANA GLACIER, ALASKA

By

Leif H. Cox

RECOMMENDED:

H. J.
Red Marsh

William E. Harrison

Keith Eslinger

Advisory Committee Chair

Paul W. Legett

Chair, Department of Geology and Geophysics

APPROVED:

D. Woodrill
Dean, College of Science, Engineering and Mathematics

W. Kan
Dean of the Graduate School

10-12-02
Date

COMPARISON OF GEODETIC AND GLACIOLOGICAL
MASS BALANCE ON GULKANA GLACIER, ALASKA

A
THESIS

Presented to the Faculty
of the University of Alaska Fairbanks
in Partial Fulfillment of the Requirements
for the Degree of

MASTERS OF SCIENCE

By
Leif H. Cox, B.S.

Fairbanks, Alaska

December 2002

ALASKA
GB
2425
A4
C69
2002

RASMUSON LIBRARY
UNIVERSITY OF ALASKA-FAIRBANKS

Abstract

The net mass balance on Gulkana Glacier has been measured since 1966 by the glaciological method, in which seasonal balances are measured at three index sites and extrapolated over large areas of the glacier. Systematic errors accumulate through time in this method; therefore the geodetic balance, in which errors are independent of time, was calculated for comparison to and possible calibration of the glaciological method. Digital elevation models (DEMs) of the glacier in 1974, 1993, and 1999 were prepared and geodetic balances computed, giving -6.0 ± 0.5 m of water equivalent (weq) from 1974 to 1993 and -11.8 ± 0.5 m weq from 1974 to 1999. These are to be compared to the glaciological balances over the same intervals, which were -5.8 ± 0.9 m weq and -11.2 ± 1.0 m weq, respectively; both balances show a tripling in thinning rate in the 1990s. These cumulative balances differ by less than 6%. For this, the glaciological method on Gulkana Glacier must be largely free of systematic errors and use a changing area altitude distribution. Relatively good contrast in the accumulation area of the glacier increased accuracy in the geodetic method.

Contents

Signature Page	i
Title Page	ii
Abstract	iii
Contents	iv
List of Figures	vi
List of Tables	vii
List of Appendices	viii
Preface	ix
1 Introduction	1
2 Methods and Results	5
2.1 Geodetic Balance	5
2.1.1 DEM Creation	5
2.1.2 Corrections	7
2.1.3 Surface Elevation Change	9
2.1.4 Errors	11
2.2 Glaciological Balance	13
3 Discussion	15
3.1 Glaciological Method Accuracy	15
3.2 Climate and Glacier Response	17
4 Conclusions	18

A Supplement to the Apex Manual	20
A.1 Before You Start	20
A.2 Terms	21
A.3 Scanning	21
A.4 Project Creation	23
A.5 Camera Calibration	23
A.6 Importing	23
A.7 Minification	24
A.8 Interior Orientation	24
A.9 Triangulation	25
A.10 Automatic Extraction	27
A.11 Quality Control and Manual Editing	28
A.12 DTM Merge	28
A.13 Exporting DTMs	28
B Camera Calibrations	30
C Archived Data	34
Bibliography	41
CD of Archived Data	Back Pocket

List of Figures

1.1	Location Map	3
1.2	Index Site, Weather Station, and Control Point Locations	4
2.1	Ablation Corrections	8
2.2	Total Emergence as a Function of Elevation	9
2.3	Surface Elevation Change in Meters of Water Equivalent	10
2.4	Glaciological Balances	14
3.1	Comparison of Cumulative Glaciological and Geodetic Mass Balances	16
C.1	Laser Altimetry Comparison	35
C.2	ELA Variations Through Time	36

List of Tables

2.1	Data Collected on Gulkana Glacier	6
2.2	Seasonal Correction Interval	7
2.3	Cumulative Geodetic and Glaciological Balances	11
2.4	DEM Accuracy	11
A.1	Strip Data Dialogue	25
B.1	1974 Aerial Camera Data	31
B.2	1993 Aerial Camera Data	32
B.3	1999 Aerial Camera Data	33
C.1	Cumulative and Net Balance at Index Sites	37
C.2	Area Altitude Distribution	38
C.3	Control Point Locations	39
C.4	Conventional and Reference Surface Cumulative Balances	40

List of Appendices

A Supplement to the Apex Manual	20
B Camera Calibrations	30
C Archived Data	34
D CD of Archived Data	Back Pocket

Preface

This main body of this thesis has been prepared for submission to the Journal of Glaciology. Rod March will be the second author on the paper. All of the glaciological data was either prepared by him or based measurements made directly by him or others in the USGS. Keith Echelmeyer and Will Harrison also spent many hours editing the paper many and helped immensely with ideas for the scientific process, but declined to be listed as authors.

Appendices are included in the thesis that contain important information which did not have a place in the paper. The first appendix is a sample work flow for creating digital elevation models (DEMs) using PCI Geomatics Apex Software. Much of the time spent working on the thesis was devoted to learning the software and creating a viable work flow preparing DEMs for differencing. Other operators will benefit from following this appendix. Also included is a CD so people working with this data will not have to reenter it by hand. All of the data on the CD is also shown in appendices because it is unknown how long the data format on the CD will be compatible with typical computers, or even how long CDs will be used.

Will Harrison contributed a great amount to this thesis and had many ideas to improve it. I learned from him that "it's the systematic errors that will kill you", and many other things not fit for a thesis. He works too hard for a man who is 'retired', but his help was greatly appreciated. Rod March had much patience helping me to find archived data and helping with my computer when it would 'crater' every week or so. Roman Motyka also read through the manuscript several times and suggested ways to improve it. Martin Truffer had the bad luck to be the only professor consistently around, so he took the brunt of my questioning during the writing, and also read the thesis numerous times. I would like to thank Keith Echelmeyer for the time he put in to help me, in spite of his adverse situation. During my time at UAF I learned an incredible amount about glaciers and climbing from him; he also tried to beat geodynamics into me, and I think some of it stuck. More importantly, he taught me about being persistent and careful in my work, and even more about life in general.

Anthony Arendt contributed so much to this paper, especially in the initial stages, that I was worried he might claim first authorship. Luckily, he already has an M. S. and claims

to not need another. Many of the other members of the lab, both students and faculty, read a version of the thesis at least once, if not many times: Carl Benson, Adam Bucki, Dan Elsberg, and Sandra Zirnheld. Thank you. I didn't give By Valentine a change to read the manuscript, but I didn't want to ruin her perpetual cheerfulness. I also did not give Craig Lingle a change to read it, but if it wasn't for him I might never have become comfortable with the kinematic surface boundary equation.

My wife, Trilby Cox, provided most of the support and funding for the non-work parts of my tenure as a masters student. Thank you so much, especially for your support the last two months of thesis writing, which we both thought might never end. I would also like to thank my parents (both sets) and my little sister, Heidi, for late night e-mails and other sources of encouragement.

This project was funded by the United States Geological Survey. Many thanks to Dennis Trabant and Rod March for securing funding, and anyone else in the USGS who helped.

Chapter 1

Introduction

Glacier-wide net mass balance is the net gain or loss of mass over an entire glacier during a given balance year; summing the net balance over a series of years results in a cumulative balance. Regional trends in cumulative mass balance are indicators of climate variability [Oerlemans and Fortuin, 1992; Hodge *et al.*, 1998; Dyurgerov and Meier, 2000] and can have a large effect on sea level [Houghton *et al.*, 2001; Arendt *et al.*, 2002]. However, world wide there are only 33 glaciers that have a balance record over 40 years in length [Dyurgerov and Meier, 1997], so one or two glaciers are often used to represent hundreds of glaciers in a region [e.g. Meier, 1984]. While region-wide extrapolations may cause inaccuracies, it has been shown that in some areas a single glacier can represent the mass balance of a region [Rabus and Echelmeyer, 1998]. A more fundamental problem is the accuracy of the limited number of mass balance records used for extrapolation.

The conventional method to measure mass balance, which we refer to as the glaciological method, relies on balance measurements made at a number of discrete points. These are then extrapolated over the glacier, usually based on the area-altitude distribution (AAD) [Østrem and Brugman, 1991]. Accumulation of errors can be problematic in this method. We are concerned primarily with systematic errors because they increase linearly with the the number of years (N) in the record, whereas random errors increase as \sqrt{N} . It is thus important to check whether the errors in the glaciological method are predominately random, or if a large systematic component is present in the given balance record.

An independent method used to check and possibly calibrate the cumulative glaciological

balance is the geodetic method [Fountain *et al.*, 1997]. In this method, maps of a glacier or their digital equivalent, digital elevation models (DEMs), are created using photogrammetry at intervals of a few years to a few decades. Differencing these DEMs, after applying corrections for density and other factors, gives the glacier-wide cumulative balance for the different time intervals. This method accounts for all spatial variability in balance, assuming the DEMs are accurate everywhere, and references a stable geographic datum.

These two methods attempt to measure the same quantity, the glacier-wide balance, but the results differ because of errors inherent in each method. Previous studies comparing the results of the two methods have found systematic errors in the glaciological method and map errors in the geodetic method. Errors in the glaciological balance have resulted from poles sinking into the snowpack, incorrectly defined previous seasonal surfaces, and/or unaccounted for internal accumulation [Krimmel, 1999; Haakensen, 1986; Conway *et al.*, 1999]. These errors will be summed over the glacier and combined with cross-glacier variations in balance from surface irregularities, avalanches, wind deposits or scours, and topographic shading [Fountain and Vecchia, 1999; Krimmel, 1999]. Such errors can accumulate systematically over time, which has been shown even to cause the glaciological balance to have the opposite sign of the geodetic balance [Conway *et al.*, 1999]. Errors associated with the geodetic method are primarily due to poor photogrammetric contrast in high accumulation areas and poor DEM registration, which in extreme cases can cause the balance to vary by several times the accepted value [Østrem and Haakensen, 1999; Andreassen, 1999]. These errors do not accumulate over time, making the cumulative geodetic balance more accurate than the cumulative glaciological balance over time scales longer than a few years. The geodetic method can thus be used to calibrate the glaciological cumulative balance [Elsberg *et al.*, 2001].

The mass balance record is especially important on Gulkana Glacier because it has one of the longest mass balance records in the United States (1966-present). It is one of three index glaciers chosen for long term balance monitoring by the United States Geological Survey (USGS) and is the only one of these index glaciers in a continental climate zone. It is often used for studies in glacier-climate interaction and sea level change [Letréguilly and Reynaud, 1989; Trabant *et al.*, 1998; Dyurgerov and Meier, 1997]. The accuracy of the glaciological balance on Gulkana Glacier has not been independently verified. Here we

determine the geodetic balance over two intervals for comparison to and possible calibration of the glaciological record.

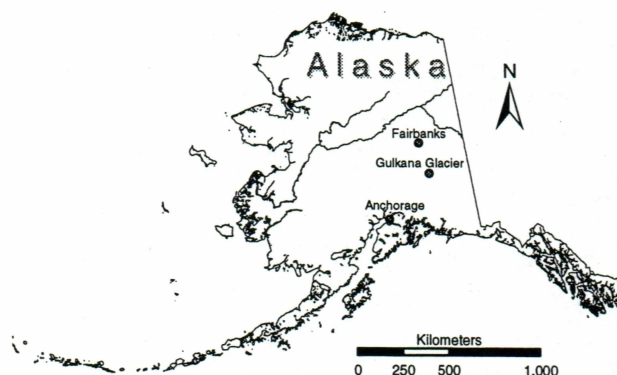


Figure 1.1. Location map.

Gulkana Glacier is located in the eastern Alaska Range ($63^{\circ} 16' \text{ N}$, $145^{\circ} 25' \text{ W}$) (Figure 1.1). It has three accumulation cirques, facing approximately south-east, south, and west, with the maximum elevation of 2450 m in the south-east facing cirque known as the Minya Basin. Ice from the three accumulation areas merges below the average equilibrium line altitude (ELA) of 1780 m and flows south to the terminus at 1200 m above sea level [March, 1998]. The terminus has retreated 3 km since its Little Ice Age maximum at the turn of the 20th century [Péwé and Mayo, 1983] and about 300 m since 1974. Glacier area has decreased from 18.4 km² in 1974 to 17.1 km² in 1999. The average balance gradient is 0.5 m a⁻¹/100 m. Air temperature and precipitation have been measured since 1967 at a weather station located on a moraine east of the lower glacier; the record is 93% complete [Kennedy et al., 1997].

Presently there are three index sites on the glacier (labeled as A, B, and D as shown in Figure 1.2) at which surface motion and mass balance have been measured by the USGS since the mid 1970's [March, 1998]. Three laser altimetry elevation profiles were flown in 1993, 1995 and 1999, and the glacier elevation profile was optically surveyed in 1993.

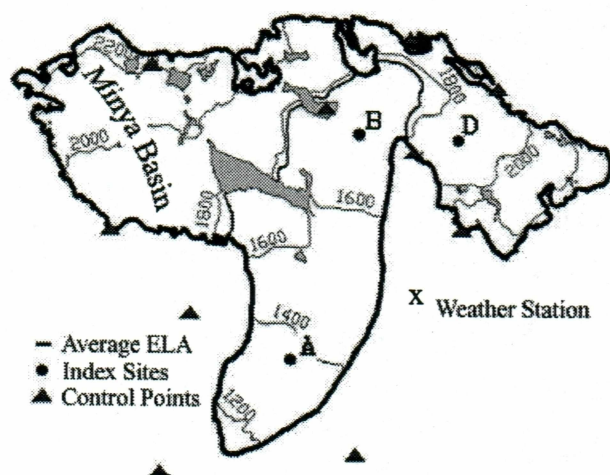


Figure 1.2. Index site, weather station, and control point locations.

Chapter 2

Methods and Results

2.1 Geodetic Balance

Geodetic balances for Gulkana Glacier were calculated using aerial photography from 1974, 1993, and 1999 (Table 2.1). (See Appendix B for camera calibrations and photography credits.) AeroMap US (Anchorage, Alaska) had previously created a high quality DEM from the 1993 photographs, but due to problems transferring control points to the 1974 and 1999 images and for increased relative accuracy, we made another DEM from the 1993 photographs. Photos taken in 1974 are high quality, but lack coverage in the upper Minya Basin, as will be discussed below.

2.1.1 DEM Creation

We generated three DEMs of Gulkana Glacier from the aerial photographs using a digital photogrammetry system (PCI Geomatics Apex). The digital process is very similar to analytical photogrammetry except that the photographs are scanned to create a digital image, the extraction of elevations is semi-automated, and a 3-D viewing system is used to edit the DEMs. Scan resolution limits accuracy, with a horizontal accuracy equal to about 1 to 2 times the ground pixel size (the ground dimension represented by one pixel) and a vertical accuracy of 0.5 to 3 times the ground pixel size [PCI, 2000].

Two types of control are used to orient images: control points, which orient the images to absolute ground coordinates, and tie points, which align the images to each other. In

Table 2.1. Data collected on Gulkana Glacier. This data was used to prepare DEMs and assess DEM accuracy.

Data Collected	Date	Number of Photographs/ Points	Photo Scale	Focal Length (mm)	Scan Res (μm)	Ground Pixel Size (m)	Remarks
Aerial Photography	9/7/1974	4	1:22000	151.293	10	0.22	Missing Minya Basin, Monochrome
Aerial Photography	7/11/1993	8	1:36000	153.211	10	0.37	Excellent Quality, Color
Aerial Photography	8/18/1999	9	1:24000	151.830	7	0.17	Poor contrast in upper basins, Monochrome
Laser Profile	6/12/1993	$\approx 10,000$					
Laser Profile	6/3/2000	$\approx 10,000$					
Optical Profile	8/1/1993	56					

1992, ten control points were surveyed to about ± 0.1 m using the Global Positioning System (GPS) (Figure 1.1); these were marked on the ground with 10 m x 10 m white crosses that were easily identified on the images acquired the following year. Images from 1974 and 1999 lacked these or any other marked control points; they were oriented using obvious features such as rock outcrops and mountain peaks. When these features are selected in multiple images they become the tie points, which allow the uncontrolled images to be aligned with controlled images. A total of 170 tie points on bedrock were used as coincident image points for this relative control.

After the images were properly controlled, an algorithm using image correlation automatically extracted DEMs on 5 m co-registered grids, which we found was optimal for image correlation. To facilitate manual editing, which was only needed on an estimated 10% of the glacier, the grids were resampled glacier-wide to a 25 m spacing. *Andreassen* [1999] has demonstrated this is a suitable grid spacing for geodetic balance calculation.

Manual editing was needed in areas of low contrast, such as the upper Minya Basin where bright snowfields display few features to be correlated. Manual editing is difficult in these areas, and care must be taken to not “float” the grid points in bright areas to a higher elevation than dark areas for lack of other information. Grids were not extracted from the 1999 Minya Basin because of poor contrast; instead, a triangulated irregular network (TIN) was used. Unlike the grid method, in which the software picks a point at every

grid node regardless of accuracy, the TIN method effectively only extracts points with an image correlation coefficient greater than a specific value. This eliminates the process of the operator manually editing thousands of inaccurate points, although some accuracy is lost because the point density may be reduced as much as an estimated ten times in very poor contrast areas.

2.1.2 Corrections

Before differencing, there are three corrections that we need to apply to each DEM to get geodetic balances that can be directly compared to the glaciological balances: ablation, emergence, and density. Ablation and emergence corrections were applied because the date of photography did not coincide with the end of the ablation season, which is when the glaciological balance is measured (see Table 2.2). We refer to these as seasonal corrections. Density corrections convert snow or ice volume to water equivalent volume change.

Table 2.2. Seasonal Correction Interval. The duration of seasonal correction is shown with the glacier wide ablation correction. Emergence corrections were applied over the same interval.

Photography Date	End of Ablation Season	Interval (days)	Glacier-Wide Ablation Correction (m weq)
9/8/1974	9/20/1974	12	-0.2
7/11/1993	9/8/1993	59	-1.8
8/18/1999	9/26/1999	39	-0.3

The ablation corrections were done following the concepts of *Reeh* [1991] using the simple degree day model of *Arendt* [1997]. Measured summer precipitation, temperature, and the DEM for each year were input into the model. The model was then tuned by varying temperature lapse rates and degree day factors to force the modeled summer balance to match the summer balance measured at each index site. Finally, the ablation in meters of water equivalent from the date of photography to the end of the balance year was calculated as a function of elevation (Figure 2.1). The 1993 corrections are relatively large, especially at low elevations, because of the long time interval and the fact that this period extended over the most intensive part of the ablation season. Internal ablation and accumulation are assumed to be negligible over the intervals.

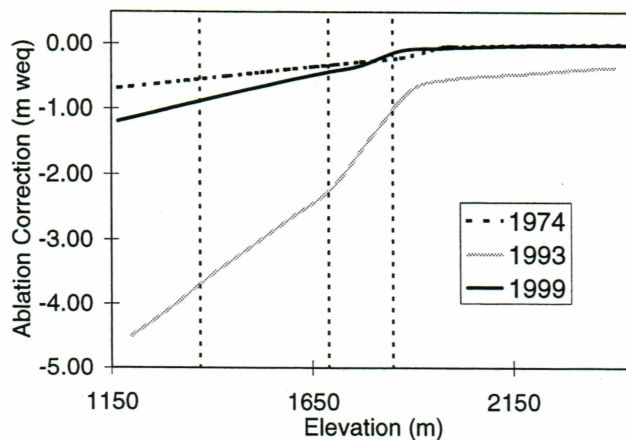


Figure 2.1. Ablation corrections. The corrections were tuned to match measured seasonal ablation at index sites represented by vertical dotted lines.

We also corrected each DEM for total emergence from the photo date to the end of the ablation season over the interval shown in Table 2.2. Any change in the surface elevation of the glacier at a point not due to ablation is due to the emergence velocity; it is the vertical component of velocity corrected for the downstream movement of ice [Paterson, 1994]. We define the total emergence to be the cumulative surface elevation change from emergence velocity over the interval. It should be noted emergence does not affect glacier-wide balance because it is merely a redistribution of mass along the entire glacier. Nevertheless, we corrected the DEMs for emergence velocity for two reasons: 1) to more accurately compare individual DEM points with optical and laser profiles (see section 2.1.4), and 2) to more accurately represent the thinning at specific areas at the end of the ablation season. A curve was fit through the total emergence measured over the interval at the index sites and adjusted to the shape of the extended mass balance curve (see section 2.2). Flow was not measured in 1974, so the average emergence from 16 years data at each index site was used. The shape of the curve from 1993 differs from the others because the measured emergence at the mid-glacier site (B) was greater than the index site low in the ablation area (Fig. 2.2).

Thickness changes of ice or snow were converted to water equivalent based on the density of the material lost or gained. The small shift in the ELA during the measurement period (Figure C.2) and the relatively small balance gradient make the assumption of Sorge's Law

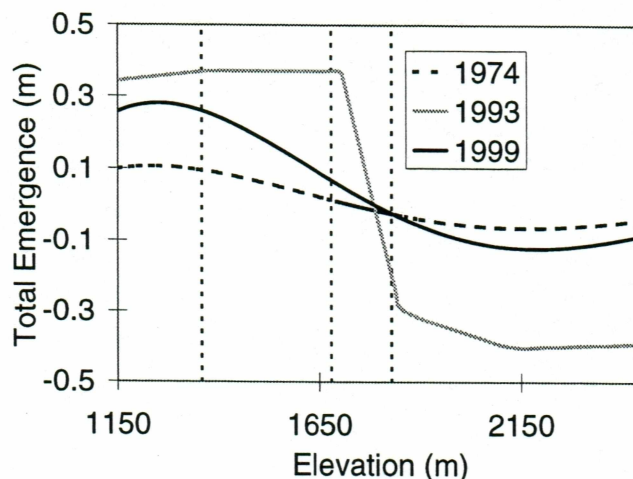


Figure 2.2. Total emergence as a function of elevation. This was measured over the correction intervals at the index sites represented by vertical dotted lines.

plausible on Gulkana Glacier. This law states that the density structure remains constant in an unchanging climate [Bader, 1954], allowing us to assume that the change in volume is related directly to water equivalent volume by the density of ice (900 kg m^{-3} , Paterson [1994]).

2.1.3 Surface Elevation Change

Surface elevation change was calculated by differencing two registered DEMs over the glacier surface. Where a surface change varied by more than 5 m from adjacent areas, the point was remeasured in the original DEM. Points where elevations could not be extracted accurately due to poor contrast were removed and the elevation change interpolated from adjacent locations. The intervals 1974 to 1993 and 1993 to 1999 were differenced, and the geodetic balance from 1974 to 1999 was simply the sum of the two intervals. Any errors in the 1993 DEM will be removed in this summation, so no inaccuracy was included.

The upper 2.7 km^2 of the Minya Basin did not contain registered grids to subtract because the 1974 photography did not cover this area and the 1999 photographs had low contrast. Thus, the 1974 to 1993 surface elevation change in the Minya Basin was extrapolated from surrounding regions. It was assumed to have no surface change because 1) the high areas of the glacier for which coverage existed showed no change over the interval and

2) the surface change of the lower Minya Basin trended to zero at the edge of coverage. The 1999 TIN in the upper Minya Basin was subtracted from coincident 1993 grid points, and the surface change was interpolated between measured points.

When all the corrections were applied, the elevation changes shown in Figure 2.3 were obtained. The cumulative geodetic balance then is equal to the glacier-wide average surface elevation change integrated over Figure 2.3. For 1974 to 1993, the geodetic balance was -6.0 ± 0.5 m weq and it was $-5.8 \pm$ m weq from 1993 to 1999. Addition of these two balances leads to a strongly negative balance over the entire interval from 1974 to 1999, as shown in Table 2.3.

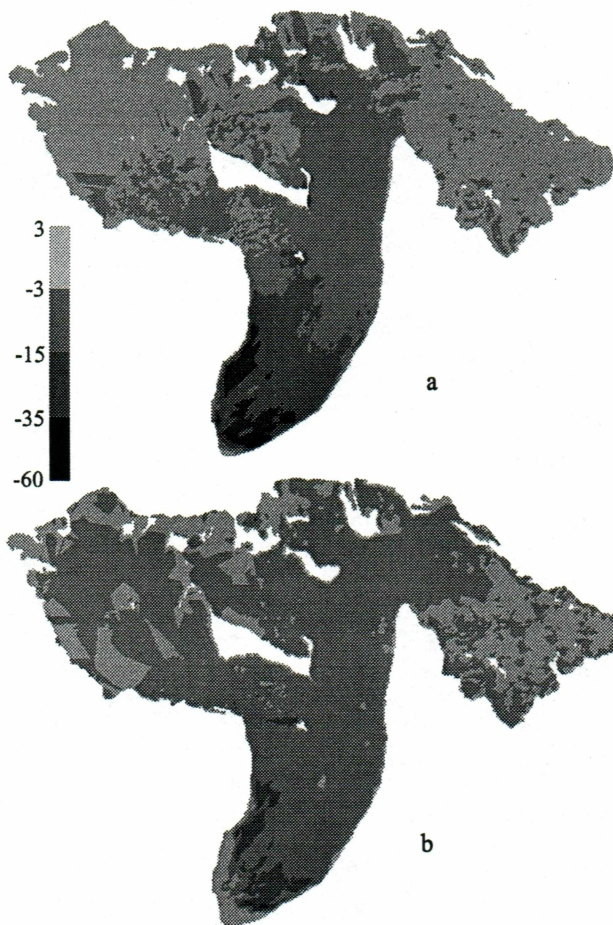


Figure 2.3. Surface elevation change in meters of water equivalent. The maps are the two intervals 1974-1993 (a) and 1993-1999 (b).

Table 2.3. Cumulative geodetic and glaciological balances.

Interval	Geodetic Balance (m weq)	Glaciological Balance (m weq)
1974-1993	-6.0 \pm 0.5	-5.8 \pm 0.9
1974-1999	-11.8 \pm 0.5	-11.2 \pm 1.0

2.1.4 Errors

Errors in the geodetic balance can result from seasonal corrections, image control, and elevation extraction—especially in the low contrast accumulation areas. Both absolute control of the DEMs to the map datum and relative control between different DEMs account for errors in image control. These are addressed separately in the following three paragraphs.

Fifty six points were surveyed on the glacier in 1993 to an accuracy of ± 0.1 m (Table 2.1). These points were well distributed over the glacier with one profile up each of the main branches and several longitudinal profiles. Each of the profiles was subjected to the same seasonal corrections as the DEMs. Comparison of DEM elevations to the optically surveyed points shows that the DEM is systematically 0.74 m weq too low (Table 2.4). There appears to be no systematic trend to the offset with elevation, although the standard deviation is greater for points in the accumulation area. The systematic difference was greater than expected, and we cannot find a satisfactory explanation for it.

Table 2.4. DEM accuracy. The standard deviation about the mean is greater over the bedrock than ice, and the relative error among DEMs is small. The standard deviation about the mean shows the accuracy of an individual measurement; this demonstrates how accurate a single point can be extracted. The standard deviation of the mean is how well the mean offset is known.

Data	Mean Offset (m weq)	Standard Deviation about the Mean (m weq)	Standard Deviation of the Mean (m weq)	Remarks
Bedrock 1993-1974	-0.20	4.70	0.22	Relative Error
Bedrock 1999-1993	-0.12	5.20	0.15	Relative Error
Optical Survey - 1993 DEM	0.74	1.34	0.20	Absolute Error
2000 Profile-1999 DEM	0.21	1.87	0.15	Absolute Error
1993 Profile-1993 DEM	0.49	1.67	0.15	Absolute Error

Airborne laser altimetry profiles flown in 1993 and 2000 were measured to an accuracy

of about ± 0.3 m [Echelmeyer *et al.*, 1996]. These profiles cover the centerline of the main branches in an almost continuous line down the glacier [Sapiano *et al.*, 1998]. The 1993 and 2000 laser altimetry profiles show the 1993 DEM to be 0.55 m weq low and 0.23 m weq low, respectively (Figure C.1). These also show no trends in the difference indicating the DEMs are not sloping relative to the datum. The mean offset is probably due to the long duration over which seasonal corrections were calculated. The important results of the profile comparisons are that the absolute accuracy of the 1993 and 1999 DEMs is less than 1 m, and that the accuracy of elevations extracted in the accumulation area are satisfactory. We did not use these independent profiles as an indication of error among the DEMs. We considered relative error to be a much better indication of this.

The relative accuracies of the DEMs were checked by subtracting two DEMs over bedrock. The relative error among DEMs is more important than the absolute error of the DEMs when calculating geodetic mass balance because it indicates the total systematic error in the geodetic balance. We note that there are several factors which may make the point measurements over bedrock less accurate than those over ice. The first problem is that the photographs were scanned to optimize contrast over the ice and snow areas making the bedrock dark (and often black) in many areas. Second, bedrock areas were not manually edited as carefully as the glacier areas. Third, except for a few locations, the only snow free areas near the upper glacier are nearly vertical causing large elevation errors from small horizontal registration errors. The increased standard deviation about the mean of the DEM over bedrock compared to measurements on the glacier illustrates these problems. In spite of the difficulties, the bedrock differencing gave encouraging results, with less than 0.3 m error among DEMs.

Our error budget for the geodetic balance includes elevation extraction, emergence corrections, density, ablation corrections, and relative orientation. *Elsberg et al.* [2001] showed that geodetic balances on South Cascade Glacier would have changed by less than 5.5% if firn is lost in the mid-elevations of the glacier instead of ice. Gulkana Glacier has experienced much less change than South Cascade Glacier over the measurement periods, so any error associated with assuming Sorge's Law will be at most a few percent. Seasonal corrections, especially in 1993, and relative orientation of the DEMs are the largest errors. These are both estimated at 0.3 m weq. Based on these estimates, we take as a conservative

estimate of the error in the geodetic balance over each interval to be ± 0.5 m weq.

2.2 Glaciological Balance

The USGS has used the glaciological method to determine the net mass balance on Gulkana Glacier every year since 1966. In this method, the end of the balance year is defined as the date of the yearly glacier-wide minimum balance. They maintained an extended stake network of up to 30 mass balance stakes until the mid-1970s, when the stake network was reduced to three index sites (see Figure 1.2) and measurements were expanded to include ice motion and surface elevation at these sites [March, 1998]. Since 1974, the balance has been calculated using data from these three index sites. The highest index site (D) is generally just above the ELA, but the ELA has been above site D three times. The seasonal balance is measured in an area 25-75 m around each pole, in an effort to reduce errors from individual snow depth soundings and small scale surface irregularities [Trabant and March, 1999].

To calculate the glacier-wide balance from the index site measurements, the glacier is divided into three elevation bins each centered at elevations halfway between the elevations of sites A and B, and sites B and D. The elevation bins are updated each year for the variations in index site altitude, but not for changes in glacier area. The map area of each elevation bin is divided by the total area of the glacier to obtain an area weighting factor. This is equivalent to using an area altitude distribution. The weighting factor is multiplied by the balance at each site and the results are summed to determine the glacier-wide surface elevation change. Estimated internal ablation from geothermal heat, ice motion, and water flowing through and under the glacier is added to the surface balance to find a glacier-wide net balance [March, 1998].

The 1967 area altitude distribution (AAD) was used to calculate the area weighting factors from 1966 to 1993. A new AAD was recalculated in 1993 by the USGS, and all subsequent balances have used the 1993 AAD. For consistency, all prior balances starting with 1966 were recalculated by the USGS with the 1993 AAD. All previously published balance measurements are therefore referenced to a fixed AAD, which effectively yields the 'reference surface' balance of *Elsberg et al.* [2001]. This balance is the appropriate variable to compare to climate, but it does not represent the true volume change and cannot be directly

compared to the geodetic balance. For this comparison, we have established time-variable AADs by calculating the area altitude distribution from DEMs of 1974, 1993, and 1999. These were then interpolated for the intervening years (see Table C.2). The glaciological balances presented in this paper are 'conventional balances' and were calculated using these time-variable AADs. Again, there is a trend toward more negative balances in the 1990s as shown in Table 2.3 and Figure 2.4. The comparison between the conventional and reference surface balances are shown in Figure 3.1 and Table C.4.

The published error for the glaciological balance on Gulkana Glacier is 0.20 m a^{-1} [March, 1998]. To verify this, the USGS calculated balances for 1966 and 1967 using both the expanded pole network and the three index sites. The expanded pole network reduces much of the balance interpolation with elevation, and the difference between the two methods was within $\pm 0.2 \text{ m a}^{-1}$. However, the expanded stake network result was not used for calibration, nor does the difference indicate whether the error is systematic or random.

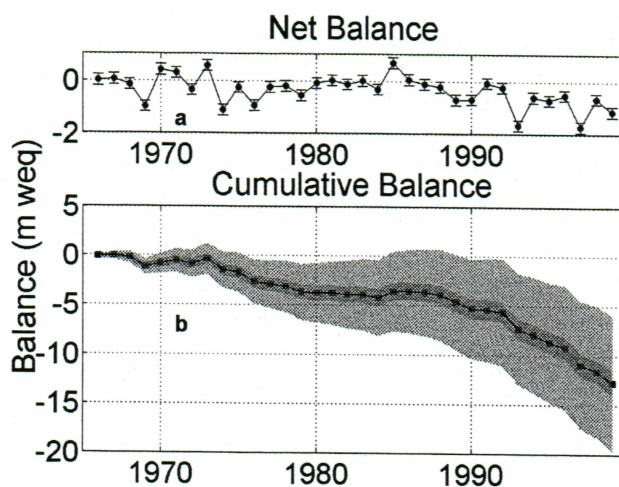


Figure 2.4. Glaciological balances: (a) net balance and (b) cumulative balance. The cumulative balance is bounded by random (dark gray) and systematic (light gray) errors of 0.2 m weq a^{-1} .

Chapter 3

Discussion

3.1 Glaciological Method Accuracy

The comparison between geodetic and cumulative glaciological balances is shown in Figure 3.1 and Table 2.3. The comparison is excellent, with the geodetic balance within the estimated error bars of the glaciological balance. This implies that the glaciological balance method on this glacier does not have large systematic errors that could arise from several sources including sinking poles, erroneous snow depths, missing internal ablation and accumulation, and an invalid area extrapolation. The USGS includes an estimated $0.05 \text{ m weq a}^{-1}$ internal ablation in the net balance. Systematically ignoring this small factor would have decreased the cumulative glaciological balance by about 10%.

On Ålfotbreen Glacier, Østrem and Haakensen [1999] placed plywood at the base of mass balance poles and observed poles forced through the plywood due to snow compaction. The USGS circumvented this problem by laying plywood or sawdust on the summer surface to unambiguously locate it the following spring by drilling or coring [Trabant and March, 1999]. In addition, single point measurements are not necessarily representative of the immediate area; deviations of 0.23 m weq in one year have been observed on three stakes less than 5 m apart [Braithwaite and Olesen, 1989]. Errors from these variations can sometimes be eliminated by sampling the balance in an area tens of meters around each index site, which the USGS does in both the ablation and accumulation season [Trabant and March, 1999].

Even with perfect point balance measurements, three poles have not typically been

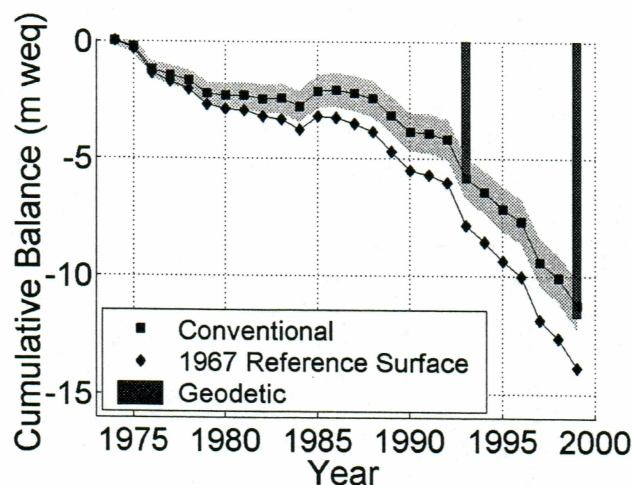


Figure 3.1. Comparison of cumulative glaciological and geodetic mass balances. The geodetic is shown to be within the random error (gray) of the glaciological balance. The 1967 reference surface balance is shown to differ from the conventional balance.

found sufficient to accurately determine the mass balance on glaciers the size of Gulkana; a minimum of 5 to 10 poles is recommended [Østrem and Brugman, 1991; Fountain *et al.*, 1997]. Krimmel [1999] found differences of 30% on the relatively small ($\approx 2 \text{ km}^2$) South Cascade Glacier, Washington, in a 27 year balance record; this was in part due to area extrapolation using between 1 and 20 poles. Our results seem to indicate that three poles are adequate to represent the balance on Gulkana Glacier. This could be due to the balance curve being well correlated across the glacier and with elevation, and the pole locations accurately represent the areas intended. But it is surprising that one index site located generally just above the ELA represents the entire accumulation area.

The reference 1967 reference surface balance differs from the actual mass change as shown in Figure 3.1. Reference surface balances are valuable, especially when relating balance to climate [Elsberg *et al.*, 2001], but must be stated as such when published because they are not the actual mass change of a glacier and cannot be directly compared to the geodetic balance and hydrologic outflow. For accurate comparisons, the conventional glaciological balance as shown in Figure 3.1 and Table 2.3 is needed. The geodetic balance can be used to correct the reference surface balance to a conventional balance using a one or two parameter fit as outlined by Elsberg *et al.* [2001].

3.2 Climate and Glacier Response

The geodetic balances correspond to an average annual thinning rate of 0.31 m a^{-1} from 1974 to 1993 and 0.96 m a^{-1} from 1993 to 1999. This accelerated thinning rate in the 1990s has been observed nearly everywhere in Alaska [Arendt *et al.*, 2002]. The more continuous cumulative glaciological balance record shows these trends as well (Figure 2.4).

The total thinning is much greater near the terminus over the first period (Figure 2.3). From 1974 to 1993, we found a maximum thinning of 60 m weq, compared to the second interval with a maximum of 40 m weq. However, during the first interval there is little change in the accumulation area, while in the second interval there was 4 m weq thinning in the accumulation area. This trend has been witnessed in most of Alaska [Arendt *et al.*, 2002]. Lower net accumulation rates in the accumulation area, accompanied by a general glacier velocity decrease, would lead to such patterns of change.

Chapter 4

Conclusions

The agreement of the two mass balance methods on Gulkana Glacier is encouraging. It supports the use of the limited number of index sites for determining the net glaciological balance if sufficient care is made in the required measurements and corrections. The glaciological mass balance of Gulkana Glacier can be accurately represented by three index sites with only one accumulation area site located just above the average ELA. This also demonstrates that the balance in a small radius can accurately describe the balance in an elevation band, and the extrapolation with elevation and area has no large systematic errors on this glacier.

This does not necessarily apply to other glaciers or even to future measurements of Gulkana Glacier. Every glaciological mass balance record needs to be regularly calibrated with the geodetic method. The relatively small error of the carefully measured glaciological balances makes them ideal for annual measurements and the time independent nature of the geodetic method makes it ideal for long term (several years to decades) measurements.

Many glaciers have featureless accumulation areas, this can account for large errors in the geodetic balances. The accumulation area on Gulkana Glacier is broken up into several small cirques with numerous nunataks and crevasses that aid stereo viewing. The snow line was also anomalously high during each year of photography, providing better contrast at high elevations. There was excellent relative control due to numerous tie points with concurrently made DEMs. Ablation corrections were calculated using a temporally and spatially tuned model.

We recommend several steps that can produce more accurate comparisons and possible calibrations of the glaciological method. The photography should be taken as close to the end of the balance year as possible; this will decrease the amount of error due to seasonal corrections and decrease the amount of snow at higher elevations, aiding stereo perception. Second, if possible, mass balance poles should be surveyed near the time of aerial photography so the balance between photography and the end of the ablation season can be determined. It is useful to have an independent profile of the glacier surface to check the DEM. A reference surface balance (which is at present published by the USGS) cannot be directly compared to actual mass change. The conventional balance, which includes changes in the total glacier area and AAD, is needed for an accurate comparison.

Appendix A

Supplement to the Apex Manual

A.1 Before You Start

Apex is a digital photogrammetry system written by PCI Geomatics [PCI, 2000]. The published manual for the software lacks an organized work flow, and some directions are ambiguous. This appendix is designed to go along with the manual, outlining the steps necessary to create accurate DEMs, and providing more detail when needed. The following will be enough to get one started and reproduce the DEMs used for this thesis. This is by no means a comprehensive manual. The scanning section should be read prior to scanning, but the rest of the sections will probably make little sense without the program running in front of you.

Apex is very finicky, it often will corrupt files and then save them upon exiting. I recommend backing up the entire data directory every time much progress has been made by copying the entire file into another directory using windows explorer. Commands are also often grayed, sometimes because a window was closed with the *x* instead of *file*→ *exit*, or sometimes it just seems to happen. This is fixed by exiting and reopening the program. Apex saves all progress automatically on exiting, so if an error is made before exiting, the data will have to be reloaded from a backed up version. There are also shortcut keys for virtually every Apex command; familiarization with these will speed repetitive processes.

Apex is well suited to creating accurate digital terrain models (DTMs), but is not effective for DTM analysis. Another program such as AutoCad with the Quicksurf addition

or ARC should be used for anything but the most basic analysis. DTM is interchangeable with digital elevation model (DEM), as used in the paper. I used DEM in the paper because it is more common in literature, but use DTM here because this is the terminology Apex uses.

A.2 Terms

Minification: The largest view without interpolation is 1:1, and each larger scale allows you to see more of the image. For each scale (e. g. 1:64) a new image is created during minification so zooming is faster.

Interior Orientation: This process corrects an image for lens distortion.

Exterior Orientation/Triangulation: This process orients an image either relative to other images or to true ground coordinates.

Console Monitor: The monitor which displays menus and is not in 3D.

Extraction Monitor: The monitor which displays in 3D.

Photograph: The picture taken by aerial photography.

Image: The digital picture after scanning.

Fiducial: Crosses or dots on aerial photographs which are used to correct for lens distortion.

A.3 Scanning

Three things are important in scanning: the resolution—typically measured in pixels per inch (ppi), the bit depth (10 bit or 8 bit), and the image orientation. The scan resolution directly affects the accuracy of the software. The horizontal accuracy of the software is 1-2 times the ground pixel size (the width in ground space of one pixel) and the vertical accuracy is 0.5 to 3 times the ground pixel size [PCI, 2000]. The ground pixel size can be

computed from the following formula:

$$PM = \left(\frac{S}{PPI}\right) \cdot \left(\frac{1}{39.37}\right) \quad (A.1)$$

where PM is the ground pixel size in meters, S is the scale, and PPI is the scan resolution in ppi [Slama, 1980]. The effectiveness of a higher scan resolution will decrease when the grain of the photographs becomes visible. Less than perfect image control and lens distortion will also decrease accuracy.

Different bit depths can be specified, with color typically scanned in 8 bit, while 10 bit is reserved for black and white. Apex currently does not use the full 10 bits for automatic extraction, but the images can be viewed and manually edited in 10 bits. This was tried with the black and white photos on Gulkana Glacier and little was gained in terms of increased contrast from 10 bit depth. The images required 4 times more memory and do not export well, so I would recommend using 8 bit depth.

The scanning orientation does matter with Apex. The images must be either scanned left or right as defined by the Apex manual. Left or right scan direction relates to the overlap region of the image. If you display the images side-by-side, the overlap must either be on the left or the right, not the top or bottom. If the photographs are scanned with incorrect orientation, it can be corrected in Apex but is time consuming. One other consideration is, as of this writing, Apex cannot handle images over 2 Gb.

When you transfer the scanned images to the computer, create a folder in the Apex directory under `apex_v70\usr\geoset\images` called 'MyProjectName'. You will need room for all the images, plus room for minified images which take up again as much room as the original images, plus about 1 Gb for other files. If there is room on the drive where Apex is located, transfer the images to the folder you just created. If there is not room on the local hard drive, the images can be put anywhere on the network.

Renaming the images to a standard convention will simplify the triangulation process. Name the first image from strip one 1_1, and the second image in the same strip name 1_2, etc. A strip is a series of images taken on one flight line, and the image number is the order the images were taken on that flight line. The numbering order of the strips does not matter, and images can be labeled in the reverse order in which they were taken.

A.4 Project Creation

Open project creation with *preparation*→ *create/edit project*. Click on *location*→ *new location*; type the project name in the first column and the path to folder you created in the second, then save it. Create the project as outline in the manual.

A.5 Camera Calibration

The camera calibration is straight forward and described well in the manual. Camera calibrations are kept on record for a long time, so they can usually be found through the organization that originally took the photos. Camera calibration used for this project can be found in Appendix B.

A.6 Importing

Once the camera calibration is entered, import the images into Apex. Select *preparation*→ *import*→ *image*→ *frame* to bring up the correct window.

1. Click on the *location* box. If the images are stored in the `apex_v70/usr/geoset/images/MyProjectName` folder, select this location. If they are stored elsewhere, create a new location as before with a new name for the location and the path directing the program to the image location.
2. From the file menu, select the correct camera calibration for the images.
3. Select *file*→ *import other*→ *image*. Browse for the image you would like to import and select it. It should be in the folder you specified in *location*.
4. This will bring up the photo data window; the coordinates refer to the location of the image corners in millimeters relative to the image center. Typically for an image with the data strip on the left, the upper left will be $x=-114$, $y=114$, and the lower right will be 114 , -114 . This is rather unimportant as interior orientation will correct any problems with this.
5. On the *create files* tab, select *support only*.

6. Go to *options* and deselect the *auto minify* option. Click *start* and the image should be imported.
7. Repeat this for all images, making sure to apply the right camera calibration if using images from different cameras, and change the location as needed.

Make sure the images have loaded properly by exiting from import and selecting in the main window, *file*→ *load images*; select view 1 and load the images. If nothing comes up, click *move to load point* in the display utility window. You will not be able to zoom out at this point. If you see nothing check the images in any kind of image viewing software to make sure they are readable.

A.7 Minification

Go to the main window again and select *preparation*→ *minification*. Select an image you want to minify it but don't click *start*. Open another minification window and select a different image. Do this with all the images, then start all. They will take about 15 minutes each. When this is finished, again load the images and make sure they are visible; this time you should be able to zoom out. Anytime you make a change to an image, you will have to close and reopen the load image window for it to load the updated image.

A.8 Interior Orientation

Use the manual interior orientation under *preparation*→ *interior orientation*→ *manual interior orientation*. Whenever picking specific points on an image use the extraction monitor. Sometimes the console monitor does not register points correctly. Locate the first two fiducials, accepting each one and then click *locate all fiducials*. Check the locations that were automatically located. You can either move the point or click *accept* and move on. The residual should be less than 1.0 according to the manual, but I haven't had luck getting the residuals below 2. Make sure you save before loading the next image.

Table A.1. Strip data dialogue. This is a guide for entering data in the table.

Current Image ID	1	The number of images in the current strip
Ref Strip ID	Current strip number minus 1 (1 if current strip is 1)	Same as previous box
Reference Image ID	1	Number of images in strip minus 1
X(along strip)	0	0
Y(across strip)	-160 (First strip enter 0)	-160 (0)

A.9 Triangulation

This is the most difficult and time consuming part of the process. It is also the most likely to corrupt files, so back up often. After every step, back up to a separate folder as outlined before. Open the triangulation window by clicking *preparation*→ *triangulation*. If working on a surface that has changed though time such as a glacier, control all the images together using bedrock and control points to tie the images. When extracting DTMs, only use images from the a single year.

Setup: Setup is the first step. This is where you tell the program where the images are in relation to one another and what algorithms to use for triangulation. For the most part, this is very straight forward if the standard naming convention was used for the images. All of the software defaults will work well.

With the naming convention used, the first number is the strip, and the second is the image in that strip. This window will be fairly straight forward to fill in, with the exception of the the strip data information. When all the rest of the fields are filled in, click the strip data button on the lower right hand of the window. This brings up a dialog which is not well explained in the manual. The numbers to write in each box are shown above in Table A.1.

To figure out the scan direction, use image loader to load the first two images of a

strip into view 1 with image 1 on the left and image 2 on the right. If the overlap region is to left of image 1, the scan direction is left. Repeat this for all the strips. Enter the correct scan direction for each strip. Up and Down do not work and will corrupt you files.

In the main triangulation window, go to *reset*→ *support file*→ *backup support*. This will back up your work. The data can be restored under the same menu. I have had problems with the backup getting corrupted, so also back up the entire data directory to another folder by cutting and pasting in windows explorer.

Exterior Initialize: Exterior initialization is the next step. Click the *initialize/solve* tab at the bottom of the triangulation window and select *exterior initialize*. You just backed up the support files, so click through the first message. Run the orientation. Now save the triangulation file and exit. Open the load imagery dialog, load image pairs (e.g. 1_1 and 1_2) one at a time, and examine the images to make sure the overlap area is approximately correct. If it is not, go to *image enhancement*→ *pairwise rectify*. If this doesn't make the images line up there is an error, probably with the scan direction. The program will let you proceed, but do not until the images are correct. Also, do not run exterior initialize after blunder detect and solve or simultaneous solve. This can cause file corruption.

Control Point Editor: Bring up the control point editor by clicking *preparation*→ *control point editor*. Now select *File*→ *Select GPF* and name a new file. Enter the control point names and coordinates, making sure to click *accept* before adding a new point. Include the accuracy because it will be used in the final triangulation solution. Save this and exit.

Interactive Point Measurement: Go back into triangulation and click on *interactive point measurement* (IPM). If many of the commands are grayed out, select view 0 in the display utility. In the IPM window, click *grnd file* and select the file that you just created in the control point editor. The IPM process is fairly straight forward and well described in the manual. Pick at least four points, control or tie, in each image, and make sure each strip is tied together with at least four points. Save and exit after picking points.

Blunder Detect and Solve: Click on *initialize/solve*→ *blunder detect and solve*. Deselect *point distribution* for now. This can be useful for checking the control and tie points distribution later, but first you want to get the images initially oriented. Click *start*. Clicking on *edit failures* will tell you which images need more tie points or if there is a bad point. You can adjust the image parallax and other parameters to make this less rigorous. Iteratively run this tool and interactive point editor until blunder detect and solve is successful. If things are not going well, check the image orientations as before with the image loader. If the images are not close to their expected relative locations, (i. e. the overlap region is not correct), you will have to reload the backed up support files and add tie points, or correct erroneous ones.

Simultaneous Solve: After blunder detect and solve has been successful, run simultaneous solve. This will perform a least square inversion on all the images simultaneously. Click on *initialize/solve*→ *simultaneous solve*. After hitting start, check the image pixel residual; the manual recommends this be lower than 1 for a final solution. If the whole solution is poor, i. e. the image residual is greater than 5, tie or control points will have to be corrected or tie points added. If it is very high (>1000) there is an erroneous data point or an error in setup. (Note that the window will not resize to accumulate large numbers, so a huge value such as 1.23456789e+120 might be interpreted as 1.23456.) If the residual is very large you will need to reload the backed up files and start again at setup. Click on *display residuals*. This displays all control and tie points in ascending order of accuracy. Points with large residuals will have to be remeasured. This can be done either from the current window or in the interactive point editor. Keep adjusting points until an acceptable solution is reached.

A.10 Automatic Extraction

Once the images are controlled, exit triangulation and click *extraction*→ *terrain*→ *automatic DTM extraction*. The setup is explained well in the manual, and the default values work well, so I will not belabor the process here. A few hints on automatic extraction. Use a spacing that results in approximately 10,000 points for the first extraction, which is small enough to run quickly and large enough to give meaningful results. Check it in the

interactive edit which is explained below. The terrain may need to be broken up into several different areas to be correctly extracted. Likely breaks between DTMs are large changes in slope or brightness (e.g., from the glacier to the valley walls). You can open several automatic extraction windows at the same time and run them overnight. I've found the best spacing to be 3-5 m. Smaller spacing does not increase accuracy, and larger spacing seems to deteriorate accuracy.

Some regions may not have enough contrast to be accurately picked by either you or the computer, so it may be beneficial to use triangulated irregular networks (TIN). The computer will effectively only pick points within a certain confidence interval when using the TIN method with heavy mass point thinning selected. This eliminates trying to edit thousands of inaccurate points in a low contrast area.

A.11 Quality Control and Manual Editing

Open *Extraction*→ *Interactive edit* and load a DTM. View each automatically extracted grid; where large areas are inaccurate, either change the grid spacing to a smaller grid, or break the area into more regions. You should not have to manually edit large parts of the DEM. Rerun inaccurate regions in automatic extraction. Once all the grids are acceptable with only small amounts of manual editing needed, use DTM merge to resample the grid to a larger grid size. I've found 25 m spacing to be accurate, but not an impossible number to manually edit; this will depend on the size of the area and the accuracy needed.

A.12 DTM Merge

Select *extraction*→ *merge*. DTM merge will resample grids to larger or smaller spacings, change the area covered by a DTM, and combine multiple DTMs. It is explained well in the manual.

A.13 Exporting DTMs

This is a fairly straight forward process outlined well in the manual. Use the xyz format to export the DTMs for evaluation in another program. Because Apex puts a header on

the exported ascii file, you may need to open the file in a text editor and erase the heading before using it in another program.

Appendix B

Camera Calibrations

Table B.1. 1974 Aerial Camera Data. This camera was used by Austin Post of the USGS to photograph Gulkana Glacier in 1974. The photographs are located in the ICA collection Geodata Center, UAF, Fairbanks, Alaska.

Camera and Lens

Camera Type

Lens Type

Camera Serial Number

KC-1B 67-208

Lens Serial Number

475

Calibrated Focal Length (mm)

151.283

Distortion Parameters

Field Angle	D _c
Degrees	(μm)
7.5	4
15	9
22.5	2
27.5	-5
30	-6
32.5	-8
35	-9
37.5	-4
40	2
42.5	0
45	-24

Principle Points

	x (mm)	y (mm)
Indicated principle point (corner fiducials)		
Indicated principle point (midside fiducials)		
Principle point of autocollimation	-0.005	-0.001
Calibrated principle point (point of symmetry)	-0.013	0.015

Fiducial Locations

Data Strip	<div><div>D</div><div>B''</div><div>A</div><div>B</div><div>C'</div><div>C</div><div>C'</div><div>B'</div></div>	A	x (mm)	y (mm)
		B	-120.350	0.000
		C	117.503	0.000
		D	-0.011	-117.804
		B'	0.010	117.591
		B''	117.409	-76.108
		C'	117.681	75.217
		C''	-76.181	-117.516
		C'''	75.119	-117.914

Table B.2. 1993 Aerial Camera Data. This camera was used by AeroMap US (Anchorage, Alaska) to photograph Gulkana Glacier in 1993.

Camera and Lens						
Camera Type	Zeiss RMK A 15/23					
Lens Type	Zeiss Pleogon A@					
Camera Serial Numer	111683					
Lens Serial Number	112649					
Calibrated Focal Length (mm) 153.211						
Distortion Parameters						
Field Angle	D _c					
Degrees	(μm)					
7.5	-2					
15	-3					
22.7	-2					
30	4					
35	2					
40	-2					
Principle Points						
	x (mm)	y (mm)				
Indicated principle point (corner fiducials)	0.010	-0.010				
Indicated principle point (midside fiducials)	-0.005	0.001				
Principle point of autocollimation	0.000	0.000				
Calibrated principle point (point of symetry)	-0.006	0.020				
Fiducial Locations						
Data Strip	3	7	2	1	x (mm)	y (mm)
				2	-103.932	-103.948
				3	103.937	103.914
				4	-103.894	103.902
	5		6	5	103.941	-103.948
				6	-113.010	-0.017
				7	112.981	0.020
	1	8	4	8	-0.020	112.981
				0.010	-112.992	

Table B.3. 1999 Aerial Camera Data. This camera was used by the Bureau of Land Management (Anchorage, Alaska) to photograph Gulkana Glacier in 1999.

Camera and Lens						
Camera Type	Wild RC8					
Lens Type	Wild Universal Aviogon					
Camera Serial Numer	485					
Lens Serial Number	UAg 263					
Calibrated Focal Length (mm) 151.83						
Distortion Parameters						
Field Angle	D _c					
Degrees	(μm)					
7.5	5					
15	7					
22.7	6					
30	0					
35	-6					
40	-7					
Principle Points						
	x (mm)	y (mm)				
Indicated principle point (corner fiducials)	-0.004	0.011				
Indicated principle point (midside fiducials)	-0.015	0.008				
Principle point of autocollimation	0.000	0.000				
Calibrated principle point (point of symmetry)	-0.007	-0.007				
Fiducial Locations						
Data Strip	3	7	2	1	x (mm)	y (mm)
	5		6	2	-106.002	-105.984
				3	106.000	106.110
				4	-106.010	106.140
				5	105.992	-105.980
				6	-110.006	0.010
	1	8	4	7	109.994	0.005
				8	-0.015	110.001
					-0.014	-109.984

Appendix C

Archived Data

93 DEM v Profiles

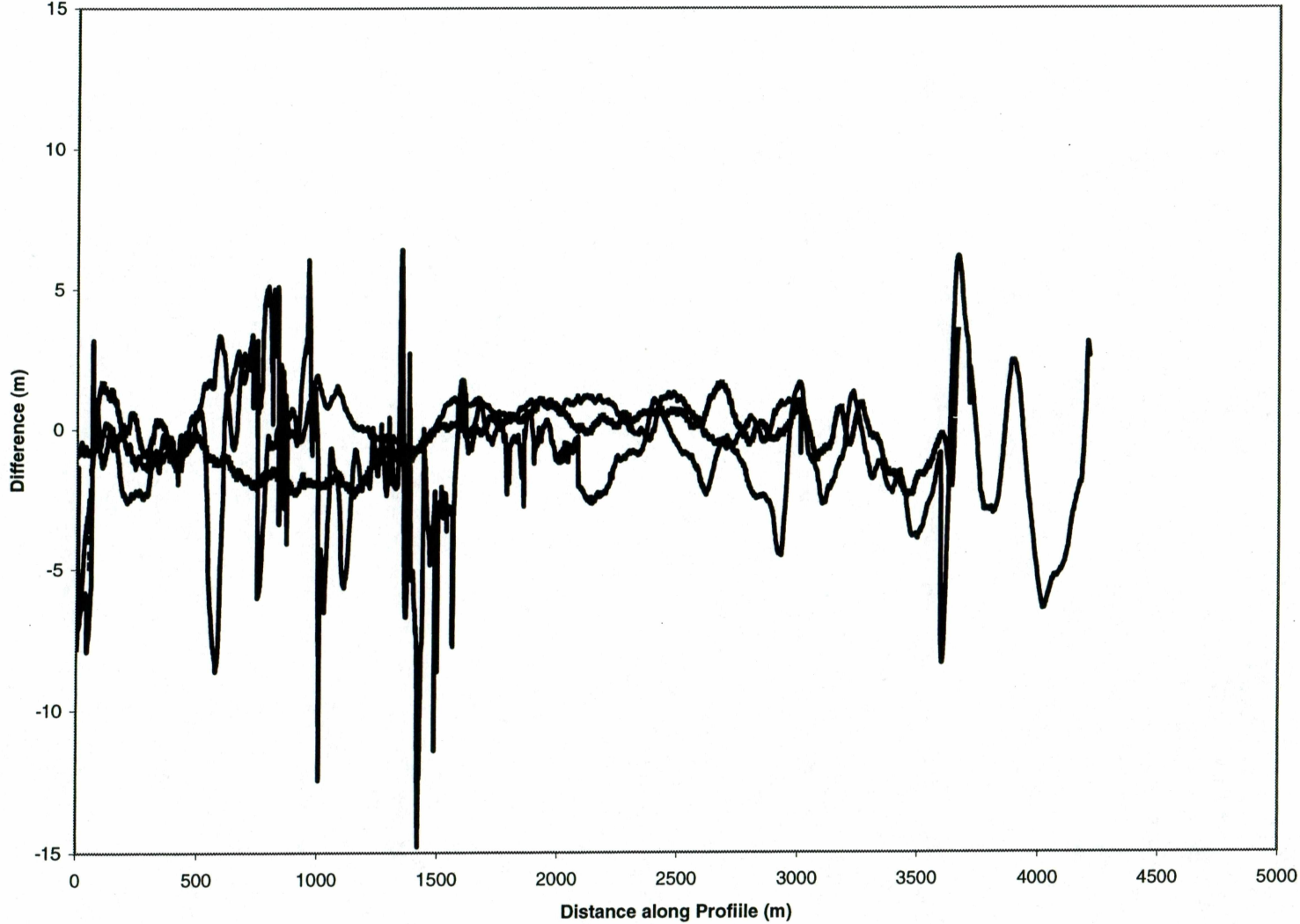


Figure C.1. Laser altimetry comparison. The differences between the seasonally corrected 1993 laser profiles and the 1993 DEM show no systematic trends with elevation.

Figure C.2. ELA variations through time.

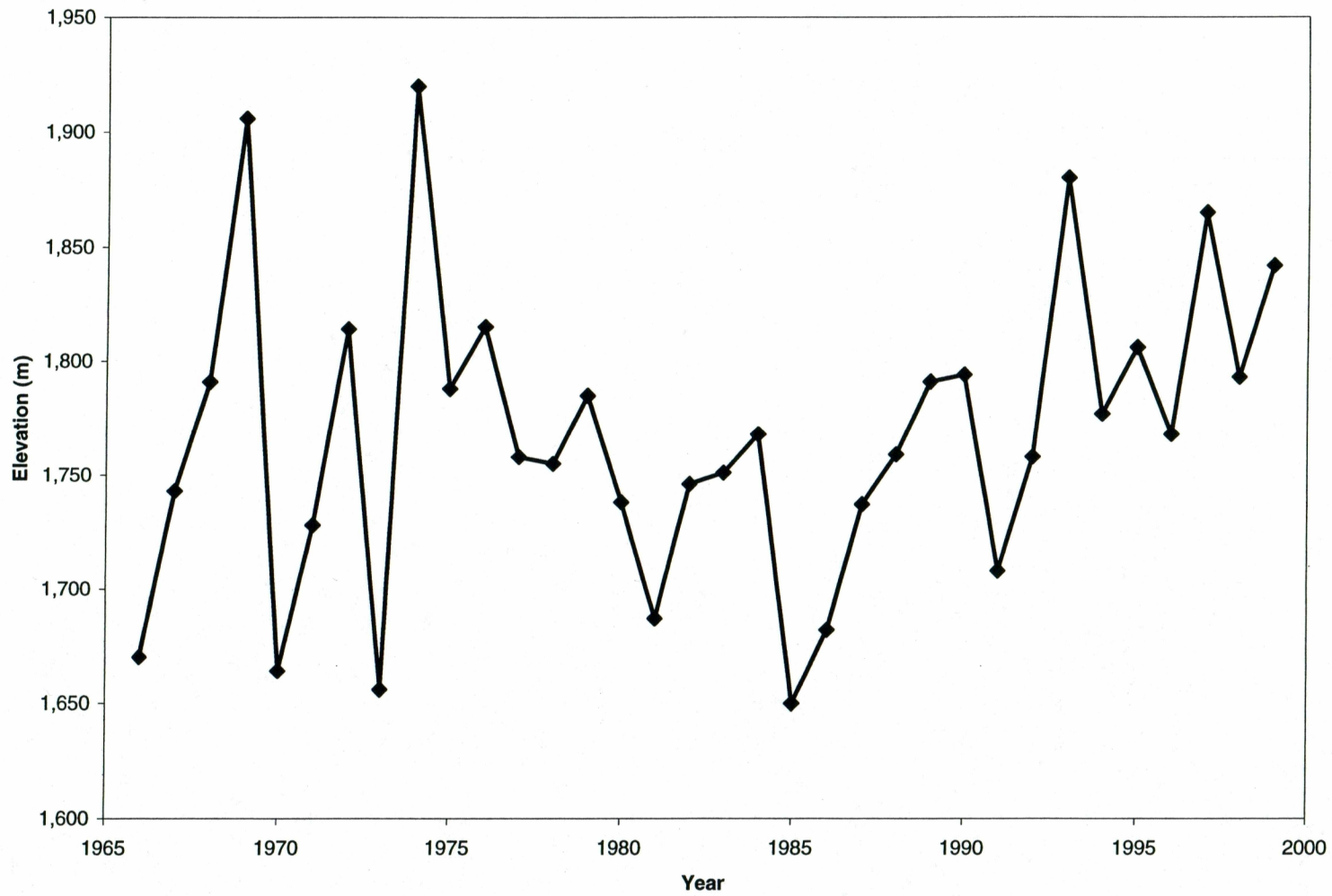


Table C.1. Cumulative and net balances at index sites. The index sites balances were measured and calculated by the USGS, and the conventional glacier-wide balances were calculated for this thesis.

Year	Net Balance (m weq)				Cumulative Balance (m weq)			
	Site A	Site B	Site D	Glacier-Wide	Site A	Site B	Site D	Glacier-Wide
1966	-2.80	0.00	0.88	-0.16	-2.80	0.00	0.88	-0.16
1967	-2.60	-0.50	1.49	0.03	-5.40	-0.50	2.37	-0.12
1968	-2.73	-1.12	1.37	-0.16	-8.13	-1.62	3.74	-0.28
1969	-3.25	-1.60	0.23	-0.99	-11.38	-3.22	3.97	-1.27
1970	-2.35	0.05	1.58	0.39	-13.73	-3.17	5.55	-0.88
1971	-1.85	-0.40	1.46	0.28	-15.58	-3.57	7.01	-0.60
1972	-2.70	-1.00	0.88	-0.36	-18.28	-4.57	7.89	-0.96
1973	-1.95	0.11	1.63	0.54	-20.23	-4.46	9.52	-0.42
1974	-3.75	-1.65	0.13	-1.12	-23.98	-6.11	9.65	-1.54
1975	-2.75	-0.55	0.84	-0.25	-26.73	-6.66	10.49	-1.80
1976	-3.85	-1.50	0.24	-0.96	-30.58	-8.16	10.73	-2.75
1977	-3.26	-0.87	0.98	-0.24	-33.84	-9.03	11.71	-3.00
1978	-3.16	-0.70	0.92	-0.22	-37.00	-9.73	12.63	-3.21
1979	-3.50	-1.26	0.66	-0.56	-40.50	-10.99	13.29	-3.77
1980	-3.10	-0.59	1.06	-0.09	-43.60	-11.58	14.35	-3.86
1981	-2.54	-0.02	0.88	0.02	-46.14	-11.60	15.23	-3.85
1982	-3.22	-0.67	1.05	-0.14	-49.36	-12.27	16.28	-3.99
1983	-3.30	-1.12	1.44	0.00	-52.66	-13.39	17.72	-3.99
1984	-3.05	-0.90	0.74	-0.34	-55.71	-14.29	18.46	-4.32
1985	-2.12	0.26	1.70	0.66	-57.83	-14.03	20.16	-3.66
1986	-3.14	0.02	1.07	0.04	-60.97	-14.01	21.23	-3.62
1987	-3.37	-0.52	1.02	-0.14	-64.34	-14.53	22.25	-3.75
1988	-3.35	-0.87	0.99	-0.23	-67.69	-15.40	23.24	-3.98
1989	-4.25	-1.43	0.64	-0.71	-71.93	-16.83	23.88	-4.69
1990	-3.95	-0.83	0.38	-0.70	-75.88	-17.66	24.26	-5.39
1991	-3.42	-0.18	0.97	-0.07	-79.30	-17.84	25.23	-5.47
1992	-2.69	-0.52	0.61	-0.24	-81.99	-18.36	25.84	-5.71
1993	-4.52	-2.54	-0.47	-1.68	-86.51	-20.90	25.37	-7.38
1994	-3.96	-0.87	0.53	-0.60	-90.47	-21.77	25.90	-7.98
1995	-3.29	-1.24	0.28	-0.72	-93.76	-23.01	26.18	-8.70
1996	-4.05	-0.82	0.61	-0.54	-97.81	-23.83	26.79	-9.23
1997	-4.99	-2.43	-0.43	-1.71	-102.80	-26.26	26.37	-10.95
1998	-3.49	-0.95	0.33	-0.66	-106.29	-27.21	26.70	-11.61
1999	-4.35	-1.35	-0.07	-1.14	-110.64	-28.56	26.63	-12.75

Gulkana Glacier Area Altitude Distribution, in square kilometers															
Year	Elevation Range (m)														Total Area
	1100	1200	1300	1400	1500	1600	1700	1800	1900	2000	2100	2200	2300	2400	
	1200	1300	1400	1500	1600	1700	1800	1900	2000	2100	2200	2300	2400	2473	
1966	0.12	0.52	1.20	1.56	1.36	2.12	2.04	2.72	2.92	2.28	1.44	0.80	0.20	0.04	19.32
1967	0.11	0.52	1.17	1.54	1.34	2.07	2.04	2.73	2.91	2.28	1.44	0.81	0.20	0.04	19.20
1968	0.11	0.52	1.15	1.52	1.32	2.02	2.04	2.74	2.91	2.28	1.43	0.81	0.20	0.04	19.08
1969	0.10	0.52	1.12	1.50	1.29	1.98	2.03	2.74	2.90	2.28	1.43	0.82	0.20	0.04	18.96
1970	0.10	0.52	1.10	1.48	1.27	1.93	2.03	2.75	2.90	2.28	1.43	0.82	0.20	0.04	18.84
1971	0.09	0.52	1.07	1.46	1.25	1.88	2.03	2.76	2.89	2.27	1.42	0.83	0.20	0.04	18.72
1972	0.09	0.52	1.04	1.44	1.23	1.83	2.03	2.77	2.89	2.27	1.42	0.83	0.20	0.04	18.60
1973	0.08	0.52	1.02	1.42	1.21	1.78	2.03	2.78	2.88	2.27	1.41	0.84	0.20	0.03	18.49
1974	0.07	0.52	0.99	1.40	1.19	1.74	2.02	2.78	2.88	2.27	1.41	0.85	0.20	0.03	18.37
1975	0.07	0.52	0.99	1.40	1.18	1.73	2.02	2.79	2.87	2.27	1.41	0.85	0.20	0.03	18.35
1976	0.07	0.52	0.98	1.39	1.18	1.73	2.02	2.80	2.87	2.27	1.40	0.86	0.21	0.03	18.34
1977	0.07	0.53	0.98	1.39	1.18	1.72	2.02	2.81	2.86	2.27	1.40	0.86	0.21	0.03	18.33
1978	0.07	0.53	0.98	1.38	1.18	1.72	2.02	2.82	2.86	2.27	1.40	0.87	0.21	0.03	18.31
1979	0.07	0.53	0.97	1.38	1.17	1.71	2.01	2.82	2.85	2.27	1.39	0.87	0.21	0.03	18.30
1980	0.07	0.53	0.97	1.37	1.17	1.71	2.01	2.83	2.85	2.26	1.39	0.88	0.21	0.03	18.28
1981	0.07	0.53	0.97	1.37	1.17	1.71	2.01	2.84	2.84	2.26	1.39	0.88	0.21	0.03	18.27
1982	0.07	0.53	0.96	1.36	1.17	1.70	2.01	2.85	2.84	2.26	1.38	0.89	0.21	0.03	18.26
1983	0.07	0.53	0.96	1.36	1.16	1.70	2.00	2.86	2.83	2.26	1.38	0.90	0.21	0.03	18.24
1984	0.07	0.53	0.95	1.35	1.16	1.69	2.00	2.86	2.83	2.26	1.37	0.90	0.21	0.03	18.23
1985	0.07	0.53	0.95	1.35	1.16	1.69	2.00	2.87	2.82	2.26	1.37	0.91	0.21	0.02	18.22
1986	0.07	0.53	0.95	1.34	1.16	1.68	2.00	2.88	2.82	2.26	1.37	0.91	0.21	0.02	18.20
1987	0.07	0.53	0.94	1.34	1.15	1.68	2.00	2.89	2.81	2.26	1.36	0.92	0.21	0.02	18.19
1988	0.07	0.54	0.94	1.33	1.15	1.68	1.99	2.90	2.81	2.26	1.36	0.92	0.21	0.02	18.18
1989	0.07	0.54	0.94	1.32	1.15	1.67	1.99	2.90	2.80	2.25	1.36	0.93	0.21	0.02	18.16
1990	0.07	0.54	0.93	1.32	1.15	1.67	1.99	2.91	2.80	2.25	1.35	0.94	0.21	0.02	18.15
1991	0.07	0.54	0.93	1.31	1.14	1.66	1.99	2.92	2.79	2.25	1.35	0.94	0.21	0.02	18.14
1992	0.07	0.54	0.92	1.31	1.14	1.66	1.98	2.93	2.79	2.25	1.35	0.95	0.21	0.02	18.12
1993	0.07	0.54	0.92	1.30	1.14	1.66	1.98	2.94	2.78	2.25	1.34	0.95	0.21	0.02	18.11
1994	0.07	0.54	0.92	1.29	1.14	1.64	1.98	2.90	2.75	2.22	1.34	0.93	0.21	0.02	17.93
1995	0.06	0.53	0.91	1.28	1.14	1.62	1.98	2.86	2.71	2.20	1.34	0.90	0.20	0.01	17.75
1996	0.06	0.53	0.91	1.27	1.14	1.61	1.98	2.82	2.68	2.17	1.34	0.88	0.19	0.01	17.58
1997	0.05	0.53	0.91	1.26	1.14	1.59	1.98	2.78	2.64	2.15	1.33	0.85	0.18	0.01	17.40
1998	0.05	0.52	0.90	1.25	1.14	1.58	1.98	2.74	2.61	2.12	1.33	0.83	0.18	0.01	17.22
1999	0.04	0.52	0.90	1.24	1.14	1.56	1.98	2.70	2.57	2.09	1.33	0.80	0.17	0.01	17.05

Table C.2. Area altitude distribution. These were as calculated by measuring the AAD in 1967, 1974, 1993, 1999 and interpolating the intervening years. The 1967 AAD is from the start of the glacier monitoring and the method used to create it is unknown.

Table C.3. Control point locations. The points were surveyed to ± 0.10 m with GPS relative to the NAD83 horizontal datum and the NGVD29 vertical datum. These were used to control the DEMs.

Site	Easting (m)	Northing (m)	Elevation (m)
Croakley	575941.34	7019451.27	2238.08
IGY	576371.37	7017131.45	2001.63
Pewe	576816.78	7012770.41	1152.70
Downdraft	577688.30	7015946.51	1600.03
Yes(L)	579330.89	7018808.42	1757.82
Blinded	579589.60	7014200.28	1676.42
Pass	580387.03	7019711.15	1909.40
Slim	580403.17	7018237.07	1910.46
Bogus	581389.55	7017035.76	2293.50
Moore	581761.29	7018815.30	2090.36

Table C.4. Conventional and reference surface cumulative balances.

Year	Convetional (m weq)	1993 Reference Surface (m weq)	1967 Reference Surface (m weq)
1966	-0.16	-0.06	-0.16
1967	-0.12	0.07	-0.14
1968	-0.28	0.02	-0.32
1969	-1.27	-0.89	-1.34
1970	-0.88	-0.44	-0.99
1971	-0.60	-0.09	-0.74
1972	-0.96	-0.40	-1.15
1973	-0.42	0.19	-0.68
1974	-1.54	-0.90	-1.88
1975	-1.80	-1.13	-2.20
1976	-2.75	-2.05	-3.25
1977	-3.00	-2.26	-3.60
1978	-3.21	-2.46	-3.91
1979	-3.77	-2.98	-4.57
1980	-3.86	-3.05	-4.77
1981	-3.85	-3.02	-4.83
1982	-3.99	-3.13	-5.08
1983	-3.99	-3.10	-5.21
1984	-4.32	-3.42	-5.64
1985	-3.66	-2.74	-5.08
1986	-3.62	-2.68	-5.14
1987	-3.75	-2.81	-5.39
1988	-3.98	-3.02	-5.74
1989	-4.69	-3.72	-6.59
1990	-5.39	-4.41	-7.40
1991	-5.47	-4.48	-7.59
1992	-5.71	-4.72	-7.92
1993	-7.54	-6.39	-9.72
1994	-8.14	-6.98	-10.43
1995	-8.86	-7.68	-11.25
1996	-9.40	-8.20	-11.90
1997	-11.11	-9.89	-13.72
1998	-11.77	-10.53	-14.47
1999	-12.91	-11.65	-15.71

Bibliography

- Andreassen, L. M., Comparing traditional mass balance measurements with long-term volume change extracted from topographical maps: A case study of Storbreen Glacier in Jotunheimen, Norway, for the period 1940-1997, *Geografiska Annaler*, 81A(4), 467, 1999.
- Arendt, A. A., *Mass Balance Modeling of an Arctic Glacier*, Masters thesis, University of Alberta, Edmonton, AB, 1997.
- Arendt, A. A., K. A. Echelmeyer, W. D. Harrison, C. S. Lingle, and V. B. Valentine, Rapid wastage of Alaska glaciers and their contribution to rising sea level, *Science*, 297, 382, 2002.
- Bader, H., Sorge's law of densification of snow on high polar glaciers, *Journal of Glaciology*, 2(15), 319, 1954.
- Braithwaite, R. J., and O. B. Olesen, Detection of climate signal by inter-stake correlations of annual ablation data Qamanârssûp Sermia, West Greenland, *Journal of Glaciology*, 35(120), 253, 1989.
- Conway, H., L. A. Rasmussen, and H. P. Marshall, Annual mass balance of Blue Glacier, USA: 1955-97, *Geografiska Annaler*, 81A(4), 509, 1999.
- Dyurgerov, M. B., and M. F. Meier, Year-to-year fluctuations of global mass balance of small glaciers and their contribution to sea-level changes, *Arctic and Alpine Research*, 29(4), 392, 1997.
- Dyurgerov, M. B., and M. F. Meier, Twentieth century climate change: evidence from small glaciers, *PNAS*, 97(4), 1406, 2000.

- Echelmeyer, K. A., W. D. Harrison, C. F. Larsen, J. Sapiano, J. E. Mitchell, J. Demallie, B. Rabus, G. Adalgeirsdottir, and L. Sombardier, Airborne surface profiling of glaciers: a case-study in Alaska, *Journal of Glaciology*, 42(142), 538, 1996.
- Elsberg, D. H., W. D. Harrison, K. A. Echelmeyer, and R. M. Krimmel, Quantifying the effects of climate and surface change on glacier mass balance, *Journal of Glaciology*, 47(159), 649, 2001.
- Fountain, A. G., and A. Vecchia, How many stakes are required to measure the mass balance of a glacier?, *Geografiska Annaler*, 81A(4), 563, 1999.
- Fountain, A. G., R. M. Krimmel, and D. C. Trabant, A strategy for monitoring glaciers, U.S. Geological Survey Circular 1132, U. S. Geological Survey, Denver, CO, 1997.
- Haakensen, M., Glacier mapping to confirm results from mass-balance measurement, *Annals of Glaciology*, 8, 73, 1986.
- Hodge, S. M., D. C. Trabant, R. M. Krimmel, T. A. Heinrichs, R. S. March, and E. G. Josberger, Climate variations and changes in mass of three glaciers in western North America, *Journal of Climate*, 11(9), 2161, 1998.
- Houghton, J. T., Y. Ding, D. Griggs, M. Noguer, P. van der Linden, X. Dai, K. Maskell, and C. Johnson, *Climate Change 2001: The Scientific Basis*, Cambridge University Press, New York, 2001.
- Kennedy, B. W., L. R. Mayo, D. C. Trabant, and R. S. March, Air temperature and precipitation data, Gulkana Glacier, Alaska, 1968-96, Water-Resources Investigations Report 97-358, U. S. Geological Survey, Fairbanks, AK, 1997.
- Krimmel, R. M., Analysis of difference between direct and geodetic mass balance measurements at South Cascade Glacier, Washington, *Geografiska Annaler*, 81A(4), 653, 1999.
- Létréguilly, A., and L. Reynaud, Spatial patterns of mass-balance fluctuations of North American glaciers, *Journal of Glaciology*, 35(120), 163, 1989.

- March, R. S., Mass balance, meteorological, ice motion, surface altitude, and runoff data at Gulkana Glacier, Alaska, 1994 balance year, Water-Resources Investigations Report 97-4251, U. S. Geological Survey, Fairbanks, AK, 1998.
- Meier, M. F., Contribution of small glaciers to global sea level, *Science*, 226(4681), 1418, 1984.
- Oerlemans, J., and J. P. F. Fortuin, Sensitivity of glaciers and small ice caps to greenhouse warming, *Science*, 258(5079), 115, 1992.
- Østrem, G., and M. Brugman, Glacier mass-balance measurements, Science Report 1, National Hydrology Research Institute, 1991.
- Østrem, G., and N. Haakensen, Map comparison of traditional mass-balance measurements: Which method is better?, *Geografiska Annaler*, 81A(4), 703, 1999.
- Paterson, W. S. B., *The Physics of Glaciers*, third ed., Pergamon, Oxford, 1994.
- PCI, *Apex version 7.0 user's manual*, PCI Geomatics, Richmond Hill, Ontario, Canada, 2000.
- Péwé, T., and L. Mayo, *Guidebook to permafrost and Quaternary geology along the Richardson and Glen Highways between Fairbanks and Anchorage, Fourth international conference on permafrost*, vol. 1, chap. Delta River Area, Alaska Range, p. 47. Alaska Division of Geological and Geophysical Surveys, 1983.
- Rabus, B. T., and K. A. Echelmeyer, The mass balance of McCall Glacier, Brooks Range, Alaska, U. S. A.; its regional relevance and implications for climate change in the Arctic, *Journal of Glaciology*, 44(147), 333, 1998.
- Reeh, N., Parameterization of melt rate and surface temperature on the Greenland Ice Sheet, *Polarforschung*, 59(3), 113, 1991.
- Sapiano, J. J., W. Harrison, and K. Echelmeyer, Elevation, volume change, and terminus retreat changes of nine glaciers in North America, *Journal of Glaciology*, 44(146), 119, 1998.

Slama, C. C., *Manual of Photogrammetry*, American Society of Photogrammetry, Falls Church, VA., 1980.

Trabant, D., R. March, and B. Kennedy, Glacier mass-balance trends in Alaska and climate-regime shifts, *Eos, Transactions, American Geophysical Union*, 79(48), F277, 1998.

Trabant, D. C., and R. S. March, Mass-balance measurements in Alaska, *Geografiska Annaler*, 81A(4), 777, 1999.